Magn Reson Med Sci 2021; 20; 76–82
doi:10.2463/mrms.mp.2019-0161
Published Online: April 7, 2020

MAJOR PAPER

Robustness of a Combined Modified Dixon and PROPELLER Sequence with Two Interleaved Echoes in Clinical Head and Neck MRI

Yutaka Shigenaga[1,2], Daisuke Takenaka[1], Tomohisa Hashimoto[1], and Takayuki Ishida[2*]

Purpose: The combination of modified Dixon (mDixon) and periodically rotated overlapping parallel lines with enhanced reconstruction sequence with two interleaved echoes, which promotes uniform fat-suppression and motion insensitivity, has recently become available for commercial magnetic resonance imaging (MRI) scanners. To compare the robustness of this combination sequence with that of standard Cartesian mDixon sequence for fat-suppressed T_2-weighted imaging in clinical head and neck MRI.

Methods: Fifty patients with head and neck tumors were involved this study. All patients underwent MRI using both the combination and standard sequences. Two radiologists independently scored motion artifacts and water–fat separation error using a 4-point scale (1, unacceptable; 4, excellent). Furthermore, comprehensive comparative evaluation was performed using a 5-point scale (1, substantially inferior; 5, substantially superior). Data were statistically analyzed using the Wilcoxon signed-rank test.

Results: In the motion artifact assessment, ratings of 3 or 4 points were assigned to 45% (observer-1, 58.0%; observer-2, 32.0%) and 97% (100%; 94.0%) of images for the standard and combination sequences, respectively ($P < 0.001$). For the water–fat separation error assessment, ratings of 3 or 4 points were assigned to 100% (100%; 100%) and 85% (84.0%; 86.0%) of images, respectively ($P < 0.001$). In the comprehensive evaluation, of the 100 cases (observer-1, 50; observer-2, 50), 96 were rated at four or five points. In cases with slight or no motion artifacts and water–fat separation errors, the combination sequence was superior to the standard sequence in term of noise and sharpness, and equal in terms of contrast.

Conclusion: Although water–fat separation errors increased significantly in the combination sequence, most of these were acceptable. The significantly decreased motion artifacts in the combination sequence significantly improved image quality overall.

Keywords: *Dixon, fat suppression, head and neck, magnetic resonance imaging, periodically rotated overlapping parallel lines with enhanced reconstruction*

Introduction

In the diagnosis of head and neck cancer, magnetic resonance imaging (MRI) is useful for evaluation of local invasion and lymph node metastases.[1–3] In particular, fat-suppressed T_2-weighted images (T_2WI) are essential for diagnosing the extent of inflammation and edema.[4] The standard Cartesian modified Dixon (mDixon) sequence, termed the TSE_mDixon_XD sequence (dedicated software developed by Philips Medical Systems, Best, The Netherlands) is a uniform water–fat separated MRI method that uses two flexible echoes, a 7-peak fat model, and water–fat shift (WFS) correction algorism.[5] It is able to acquire uniform fat-suppressed images even in high B_0 inhomogeneity regions, such as the oral and nasal cavities and the pharynx, compared with other fat suppression techniques.[6–8] However, this sequence is more sensitive to patient motion and pulsatile blood flow than are other fat suppression techniques, because it requires two echo times (TE) and repetition time (TR).[9] As a measure against motion artifacts, the periodically rotated overlapping parallel lines with enhanced reconstruction (PROPELLER) method has been reported.[10–12] Recently, several methods for combining Dixon

[1]Department of Radiology, Hyogo Cancer Center, Hyogo, Japan
[2]Division of Health Sciences, Graduate School of Medicine, Osaka University, Osaka, Japan

*Corresponding author: Division of Health Sciences, Graduate School of Medicine, Osaka University, 1-7, Yamadaoka, Suita, Osaka 565-0871, Japan. Phone: +81-6-6879-2573, Fax: +81-6-6879-2573, E-mail: tishida@sahs.med.osaka-u.ac.jp

Received: November 6, 2019 | Accepted: March 3, 2020

water–fat separation and PROPELLER motion correction have been reported.[13–15] At last, the combination of the mDixon and PROPELLER sequences with two interleaved echoes, proposed by Schär et al.,[15] has become available for commercial MRI scanners, and is termed the TSE_mDixon_MultiVane_XD sequence (dedicated software developed by Philips Medical Systems, Best, The Netherlands). However, to our knowledge, the robustness and usefulness of this sequence have not yet been proven in a clinical setting.

According to previous study by Schär et al.,[15] the TSE_mDixon_MultiVane_XD sequence is designed to achieve both uniform water–fat separation and robustness to motion. Unlike the TSE_mDixon_XD sequence, two flexible echoes are acquired by shifting the acquisition window between odd and even echoes within one TR. Thus, both TE_1 and TE_2 blades are acquired simultaneously by a single shot, making it insensitive to motion. The Dixon water–fat separation is performed for each TE_1 and TE_2 pair with a B_0 map; which acquire water-only and fat-only blades, and correct the WFS. The motion correction algorism, which was developed based on the modified PROPELLER method,[11] is then performed. In addition, use of a parallel imaging technique, sensitivity encoding (SENSE),[16] leads to shorter scanning time and wider blade width.[12] Therefore, the blade width is equal to the TSE factor times the SENSE factor divided by two. When setting scan parameters, the shot per blade and TSE factor are limited to only 1 and 16 or more, respectively, meaning that only T_2WI can be acquired.

We hypothesized that, in clinical cases with head and neck tumors, the TSE_mDixon_MultiVane_XD sequence would yield decreased motion artifacts due to swallowing, breathing, etc., at a uniform fat-suppression, as compared with the TSE_mDixon_XD sequence. Thus, we here investigated whether the TSE_mDixon_MultiVane_XD sequence was more robust in fat-suppressed T_2WI of the head and neck than the TSE_mDixon_XD in clinical cases.

Materials and Methods

Study patients

This study population consisted of 50 consecutive patients (5/2017–10/2017) who underwent head and neck MRI for diagnosis of tumor and follow-up in our institution and who agreed to participate in this study. Patient characteristics are presented in Table 1.

The prospective cross-sectional study was approved by the local Institutional Review Board, and written informed consent was obtained from all subjects.

Magnetic resonance imaging

In this study, a 3T MR system (Ingenia Release 5.3; Philips Medical Systems, Best, The Netherlands), equipped with a 20-channel head and neck coil, was used. All patients underwent conventional routine MRI, including the T_2W_TSE_mDixon_XD (T_2W_mD) sequence, to which the T_2W_TSE_mDixon_MultiVane_XD (T_2W_mD_MV) sequence was added consecutively. In order to exclude fatigue and familiarity bias, patients were randomly assigned to the T_2W_mD sequence-first group or T_2W_mD_MV sequence-first group, using computer-based randomization in advance. Before each scan, patients were given a short break of approximately 15 s, were told next scan duration, and were instructed not to move.

Table 1 Patient characteristics

Characteristics	*N* = 50
Sex, *n* (%)	
Men	34 (68)
Women	16 (32)
Age, years	
Median (interquartile range)	68.5 (61–76)
Body mass index, kg/m^2	
Median (interquartile range)	20.9 (19.0–22.7)
Tumor location, *n* (%)	
Oral cavity	33 (66)
Pharynx	11 (22)
Larynx	3 (6)
Salivary gland	2 (4)
Thyroid	1 (2)

The detailed typical scan parameters are summarized in Table 2. In the T_2W_mD_MV sequence, the TSE factor and SENSE factor were set to 32 and 2.5 respectively in order to widen the blade width and shorten the scan time. The increased TSE factor expanded the shot duration time, extended the TE, and caused increasing blur. To improve these problems, the echo spaces were reduced by widen bandwidth, and the TE-equivalent value was made equal to the T_2W_mD sequence by setting the refocusing angle to 90°. The lower refocusing angle establishes pseudo steady state rapidly, which is able to shorten the TE-equivalent value and suppress blur.[17] The regional saturation band was placed on the inferior side to minimize pulsatile blood-flow artifacts. Depending on the tumor size and the extent of inflammation, the slice thickness, inter-slice gap, and number of slices were appropriately changed (from 3 to 6 mm, 10% to 20%, and 20 to 50 slices). Finally, the SENSE factor was adjusted in the T_2W_mD sequence and MultiVane% was adjusted in the T_2W_mD_MV sequence so that the scan time remained the same. Because we thought extending the scan time can increase the risk of exposure to patient movement.

Image quality evaluation

The T_2W_mD_water and T_2W_mD_MV_water data sets were visually assessed in a random order on a workstation (SYNAPSE VINCENT; Fujifilm Co., Tokyo, Japan) by two experienced radiologists (observer-1, 11 years; observer-2, 30 years), independently. Both observers were unaware of patient information and sequence parameters. Adjustment of the

Table 2 Scan parameters

	T_2W_mD sequence	T_2W_mD_MV sequence
Slice orientation	Transverse	Transverse
FOV (mm)	240	240
Acquisition voxel size (mm)	0.88/0.89/5.00	0.88/0.88/5.00
Reconstruction voxel size (mm)	0.47/0.47/5.00	0.47/0.47/5.00
Slice thickness (mm)	5	5
Slice gap	0.5	0.5
Slices	30	30
Fold-over direction	AP	-
SENSE reduction factor	1.5	2.5
TSE factor	18	32
Startup echoes	1	0
Profile order	linear	linear
TSE echo space/shot duration time (ms)	8.6/163	6.5/208
Water–fat shift (pix)/ Bandwidth (Hz/pixel)	0.709/612.7	0.614/707.0
Flip angle (°)	90	90
Refocusing control	constant	constant
Angle (°)	120	90
Act. TR (ms)	3500	3500
Act. TE (ms)	90	107 (104/111)
TE-equivalent (ms)	80	80
REST slabs	1(inferior)	1(inferior)
MultiVane percentage (%)	–	300
Shots per blade	–	1
MultiVane gross motion correction	–	yes
NSA	1	1
Packages	2	2
Total scan time	02:27	02:34

TSE, turbo spin echo; TR, repetition time; TE, echo time; FA, flip angle; FOV, field-of-view; NSA, number of signals averaged; SENSE, sensitivity encoding; mD, mDixon_XD; MV, MultiVane_XD; REST, regional saturation.

window-level and -width was allowed during their assessments. The range of assessment was from below the basicranium to the hypopharynx level. Brain and aliasing artifacts from the shoulder, a PROPELLER-specific error,[18] were not evaluated.

First, the motion artifacts and water–fat separation errors were assessed using a 4-point scale: 1 = unacceptable, diagnosis impossible due to severe artifact; 2 = poor, diagnosis possible although artifacts are present; 3 = good, artifacts slightly discernible; 4 = excellent, no artifacts. Second, for image quality evaluation in cases without motion artifacts and water–fat separation error, assessments of noise, sharpness, and contrast were added for cases that both observers assessed scored 3 or 4 points in both above artifact assessments. Two data sets were randomly toggled on the left or right side for blind review, and evaluated using the following 5-point scale: 1 = left images are substantially better than the right images; 2 = left images are better than the right images; 3 = left images are the same as the right images; 4 = left images are worse than the right images; 5 = left images are substantially worse than the right images. Finally, in all cases, it was evaluated which images were preferable overall for diagnosis using this 5-point scale.

Statistical analysis

Normality of the distribution of the tested variables was analyzed with the Shapiro–Wilk test. Continuous variables are presented as median and quartiles for non-normally distributed variables, and categorical variables are expressed as absolute and relative frequencies (%). The motion artifact and water–fat separation error ratings were compared using the Wilcoxon signed-rank test. $P < 0.05$ was considered statistically significant. These statistical analyses were performed with SPSS software, release 23.0 (SPSS Inc., Chicago, IL, USA).

Linear weighted κ-coefficients were calculated using Excel to assess the inter-observer agreement. The κ-value is typically interpreted as an indication of no agreement when it is <0, as slight agreement when κ is 0–0.2, as fair agreement when κ is 0.2–0.4, as moderate agreement when κ is 0.4–0.6, substantial agreement when κ is 0.6–0.8, and almost perfect agreement when κ is 0.8–1.0.

Results

Table 3 summarizes the results of assessment for motion artifact and water–fat separation error. In the motion artifact

Table 3 Artifact score by observer and technique

	Observer-1		Observer-2	
	mD	mD_MV	mD	mD_MV
Motion artifact				
Excellent	6 (12%)	45 (90%)	2 (4%)	33 (66%)
Good	23 (46%)	5 (10%)	14 (28%)	14 (28%)
Poor	14 (28%)	0	17 (34%)	3 (6%)
Unacceptable	7 (14%)	0	17 (34%)	0
P-value	<0.001		<0.001	
κ-coefficients	0.83			
Water–fat separation error				
Excellent	48 (96%)	21 (42%)	48 (96%)	30 (60%)
Good	2 (4%)	21 (42%)	2 (4%)	13 (26%)
Poor	0	5 (10%)	0	2 (4%)
Unacceptable	0	3 (6%)	0	5 (10%)
P-value	<0.001		<0.001	
κ-coefficients	0.92			

mD, modified Dixon_XD; MV, MultiVane_XD.

score, good or excellent ratings (scores of 3 or 4) were assigned to a mean of 45% of the T_2W_mD sequence images (observer-1, 58.0%; observer-2, 32.0%). In contrast, of those obtained with the T_2W_mD_MV sequence, on average 97% (observer-1, 100%; observer-2, 94.0%) had good or excellent ratings. The motion artifact score was rated significantly higher on T_2W_mD_MV sequence images than on T_2W_mD sequence images ($P < 0.001$). The water–fat separation error score from the T_2W_mD sequence was good or excellent in all cases. On the other hand, those from the T_2W_mD_MV sequence was good or excellent in approximately 85% of images (observer-1, 84.0%; observer-2, 86.0%). There was a significant difference between the T_2W_mD sequence and T_2W_mD_MV sequence in terms of water–fat separation error score ($P < 0.001$). For inter-observer agreement, the calculated linear weighted κ-coefficients were 0.83 and 0.92 for motion artifact and water–fat separation error scores, respectively, indicating almost perfect agreement.

Representative cases of the T_2W_mD sequence and the T_2W_mD_MV sequence are shown in Fig. 1. Motion artifact was substantially improved, although a slight water–fat separation error is observed for subcutaneous fat. In addition, typical cases with unacceptable water–fat separation error in the T_2W_mD_MV sequence are shown in Fig. 2. All severe water–fat separation errors were observed in images of a relatively raised jaw.

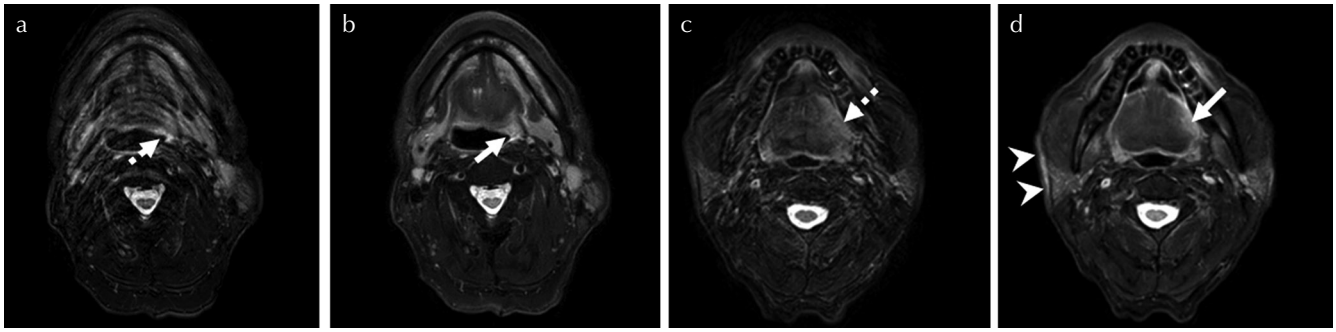

Fig. 1 Comparison between T_2W_mD sequence and T_2W_mD_MV sequence. Upper panel: The pharynx in a 63-year-old male patient with oropharynx squamous cell carcinoma before treatment. Lower panel: The oral cavity in a 68-year-old male patient with oral tongue squamous cell carcinoma before treatment. The T_2W_mD sequence shows severe motion artifacts which cover signal changes [(**a** and **c**) dotted arrows]. The T_2W_mD_MV sequence shows no motion artifact; thus, the tumor signals are observed clearly [(**b** and **d**) arrow]. However, in the T_2W_mD_MV sequence, water–fat separation errors occurred in a portion of subcutaneous fat [(**d**), arrowhead]. T_2W, T_2-weighted image; mD, modified Dixon_XD; MV, MultiVane_XD.

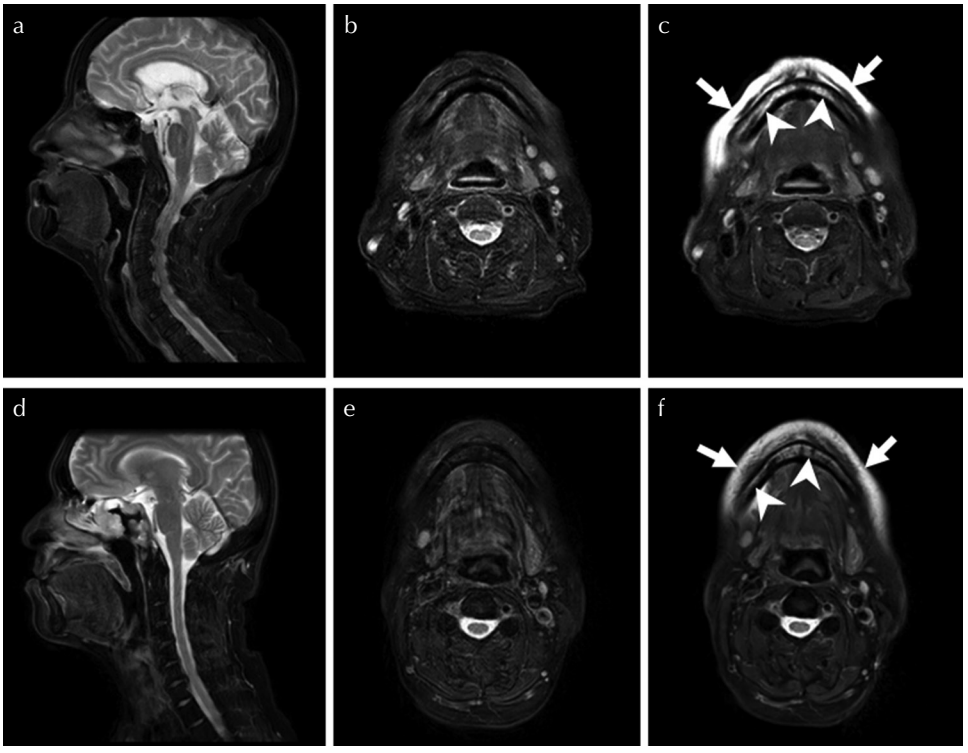

Fig. 2 Unacceptable water–fat separation error in the T_2W_mD_MV sequence. Upper panel: An 88-year-old female patient with postoperative recurrence of buccal mucosa squamous cell carcinoma. Lower panel: A 47-year-old male patient with nasopharynx squamous cell carcinoma after radiation-chemotherapy. (**a** and **d**) Sagittal image from T_2W_mD sequence. (**b** and **e**) Transverse image at the level of the jaw from T_2W_mD sequence. (**c** and **f**) Transverse image at the level of the jaw from T_2W_mD_MV sequence. A severe water–fat separation error is observed on not only subcutaneous fat [(**c** and **f**) arrows], but also mandibular marrow [(**c** and **f**) arrowheads]. T_2W, T_2 weighted image; mD, modified Dixon_XD; MV, MultiVane_XD.

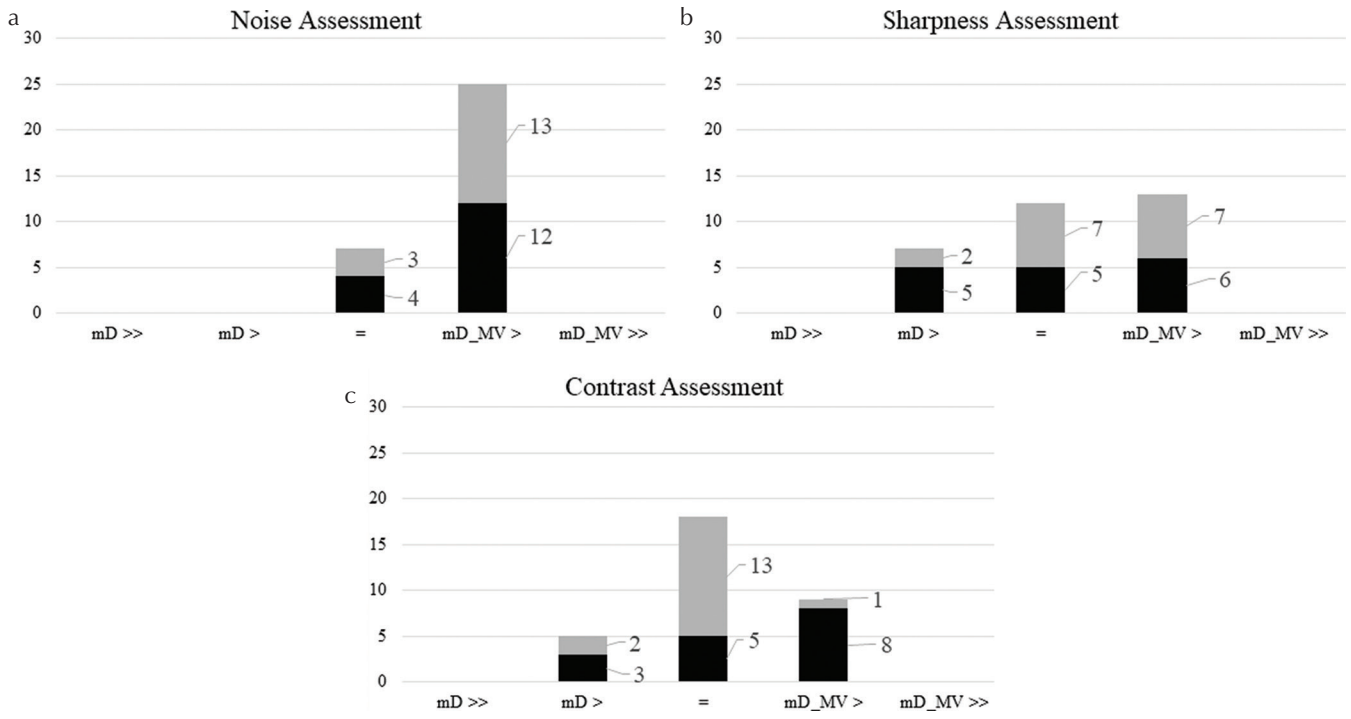

Fig. 3 Image quality assessment between T_2W_mD sequence and T_2W_mD_MV sequence in cases with slight or no motion artifact and water–fat separation error. (**a**) Noise assessment. (**b**) Sharpness assessment. (**c**) Contrast assessment. Each bar graph shows a comparison of 16 cases by the two respective observers. The five categories correspond to the T_2W_mD_MV sequence being substantially better or worse than (>>), better or worse than (>), or equal to (=) the T_2W_mD sequence. Grey and black colors represent the two radiologists' comparisons, respectively. T_2W, T_2-weighted image; mD, modified Dixon_XD; MV, MultiVane_XD.

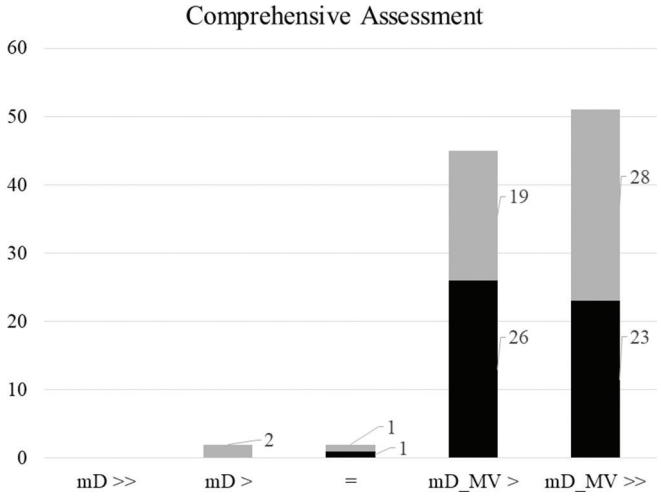

Fig. 4 Comprehensive comparative assessment between the T_2W_mD sequence and T_2W_mD_MV sequence. Bar graph shows a comparison of all cases by the two respective observers. The five categories correspond to the T_2W_mD_MV sequence being substantially better or worse than (>>), better or worse than (>), or equal to (=) the T_2W_mD sequence. Grey and black colors represent the two radiologists' comparisons, respectively. T_2W, T_2-weighted image; mD, modified Dixon_XD; MV, MultiVane_XD.

Figure 3 shows the results of comparative assessments of noise, sharpness, and contrast in the cases with slight or no motion artifact and water–fat separation error. In terms of noise, the T_2W_mD_MV sequence was superior to the T_2W_mD sequence (Fig. 3a). In terms of sharpness, the T_2W_mD_MV sequence was slightly superior to the T_2W_mD sequence (Fig. 3b). In terms of contrast, these sequences were almost equivalent (Fig. 3c).

Figure 4 shows the results of the overall comparative evaluation. The T_2W_mD_MV sequence was superior to the T_2W_mD sequence in almost cases (observer-1, 94.0%; observer-2, 98.0%; $\kappa = 0.92$).

Discussion

In this study, we compared the robustness of the newly available combination sequence with that of standard Cartesian mDixon sequence for fat-suppressed T_2WI of the head and neck in a clinical context. Our main finding was that the T_2W_mD_MV sequence improved motion artifacts and deteriorated water–fat separation error compared with the T_2W_mD sequence.

In this study, both observers scored some cases as having unacceptable motion artifacts for diagnosis on the T_2W_mD

sequence. The T_2W_mD sequence is sensitive to patient motion as it requires two flexible echoes across TR. Additionally, a higher magnetic field tends to deteriorate the motion artifacts.[19] These drawbacks are critical in head and neck MRI because motion in this region occurs frequently due to swallowing, breathing, etc. In contrast, neither observer found any cases with unacceptable motion artifact for diagnosis on the T_2W_mD_MV sequence images. The T_2W_mD_MV sequence does not require multiple TRs as it acquires two echoes interleaved in each shot.[15] Furthermore, the modified PROPELLER algorism makes this approach more insensitive to patient motion. While, with the T_2W_mD_MV sequence, water–fat separation error was more frequently observed than with the T_2W_mD sequence. Although most of them were confined to a portion of subcutaneous fat and were acceptable for diagnosis, in a few cases, an unacceptable water–fat separation error was observed. All severe water–fat separation errors were observed on a relatively raised jaw, suggesting that they were caused by large B_0 inhomogeneities. The Dixon water–fat separation needs precision B_0 map. In the T_2W_mD sequence, the B_0 map is produced in each slice. On the other hand, in the T_2W_mD_MV sequence, the B_0 map is produced in each low-resolution blade. Schär et al.[15] described that water–fat swaps may occur in some of blades partly due to the low resolution in the phase encoding direction, and level of artifacts depend on how many affected blades. Therefore, we consider that severe water–fat separation errors in raised jaw result from all or almost blades water–fat swaps. Schär et al.[15] have shown that combination of the mDixon and PROPELLER sequence with two interleaved echoes is superior for fat-suppressed T_2WI as compared with the spectral fat-saturated standard PROPELLER sequence. Our study showed that the combination of mDixon and PROPELLER sequences is inferior to the standard mDixon sequence in terms of fat suppression. However, this unacceptable water–fat separation error may be resolved by making B_0 inhomogeneities smaller with a simple method, such as ensuring that the patient's chin is lowered.

We had originally hypothesized that, in cases without motion artifact and water–fat separation error, the T_2W_mD_MV sequence would lead to a slight blur, low noise, and equivalent contrast compared with the T_2W_mD sequence. The T_2W_mD_MV sequence has non-filled *k*-space corners and an oversampled *k*-space center,[10,11] and the TE-equivalent value was adjusted to equal by lowering the refocusing pulse. These hypotheses were consistent with the study results in terms of noise and contrast. However, in terms of sharpness, the T_2W_mD_MV sequence was slightly superior to the T_2W_mD sequence. This may be due to the use of a criterion of "motion artifact score of 3 or 4 points," because deteriorated sharpness was attributed to even a slight motion artifact. Although it might have been better to assess images using only a motion artifact score of 4 points, the number of cases assigned a score of 4 was too small to allow comparison [observer-1, six cases (12%); observer-2, two cases (4%)]. If the influence of motion artifacts was completely excluded, result of sharpness assessment may reverse since the T_2W_mD sequence has filled *k*-space corners compared with the T_2W_mD_MV sequence. However, in these three assessments, there was no case that T_2W_mD_MV sequence were substantially worse than the T_2W_mD sequence. These results convince us that T_2W_mD_MV sequence does not critically deteriorate image quality to undiagnosable level.

In the comprehensive comparative evaluation, both observers assessed that the T_2W_mD_MV sequence was preferable for diagnosis compared with the T_2W_mD sequence in almost cases. This result suggests that the degree of motion artifact is particularly important among various image quality assessment factors. Therefore, the comprehensive evaluation was influenced substantially by the robustness to patient motion.

Our study had some limitations. First, although image assessments were performed in blinded manner, experienced radiologists might recognize what sequence was applied. Second, only visual assessment was performed, and physical assessment was not performed. In this study, noise measurement was difficult, since many of the acquired clinical images had motion artifacts; furthermore, using parallel imaging and a radial sampling technique complicated the appearance of noise. Therefore, it was impossible to compare image quality accurately using the signal-to-noise ratio or contrast-to-noise ratio. Third, in assessments of noise, sharpness, and contrast, the influence of motion artifacts could not be completely excluded. The possibility that the findings of those assessments would differ if sample size was larger and the influence of motion artifacts was completely excluded cannot be ruled out. Especially, result of sharpness assessment will almost certainly reverse. Finally, sensitivity and specificity were not calculated by receiver operating characteristic (ROC) curve analysis. It is difficult to perform ROC analysis in this context, because there are few opportunities to scan normal patients due to our institution's policies. Thus, these points may need to be studied further. However, the observed significant reduction in motion artifacts suggests that we accomplished the purpose of this study, which was to investigate the robustness of the new combined sequence.

Conclusion

For acquiring fat-suppressed T_2WI of the head and neck in clinical cases, the combination of mDixon and PROPELLER sequences with two interleaved echoes increased the water–fat separation error, as compared with the standard Cartesian mDixon sequence. However, this sequence decreased motion artifacts significantly and improved overall image quality, suggesting its potential for enhancing diagnostic performance.

Conflicts of Interest

None of the authors has any conflicts of interest regarding this study.

References

1. Bolzoni A, Cappiello J, Piazza C, et al. Diagnostic accuracy of magnetic resonance imaging in the assessment of mandibular involvement in oral-oropharyngeal squamous cell carcinoma: a prospective study. Arch Otolaryngol Head Neck Surg 2004; 130:837–843.
2. Stuckensen T, Kovács AF, Adams S, Baum RP. Staging of the neck in patients with oral cavity squamous cell carcinomas: a prospective comparison of PET, ultrasound, CT and MRI. J Craniomaxillofac Surg 2000; 28:319–324.
3. Liao LJ, Lo WC, Hsu WL, Wang CT, Lai MS. Detection of cervical lymph node metastasis in head and neck cancer patients with clinically N0 neck-a meta-analysis comparing different imaging modalities. BMC Cancer 2012; 12:236.
4. Morimoto Y, Tanaka T, Kito S, et al. Instability of background fat intensity suppression using fat-saturated (FS) MR imaging techniques according to region and reconstruction procedure in patients with oral cancer. Oral Oncol 2004; 40:332–340.
5. Perkins TG, Duijndam A, Eggers H, de Weerdt E, Rijckaert YHE. The next generation fat-free imaging. Available from: https://philipsproductcontent.blob.core.windows.net/assets/20170523/77840f58014b4ea8bc44a77c015697b7.pdf (Accessed: Oct 6, 2019).
6. Eggers H, Börnert P. Chemical shift encoding-based water-fat separation methods. J Magn Reson Imaging 2014;40: 251–268.
7. Hahn S, Lee YH, Suh JS. Detection of vertebral metastases: a comparison between the modified Dixon turbo spin echo T_2 weighted MRI and conventional T_1 weighted MRI: a preliminary study in a tertiary centre. Br J Radiol 2018; 91:20170782.
8. Pokorney AL, Chia JM, Pfeifer CM, Miller JH, Hu HH. Improved fat-suppression homogeneity with mDIXON turbo spin echo (TSE) in pediatric spine imaging at 3.0T. Acta Radiol 2017; 58:1386–1394.
9. Ma J, Jackson EF, Kumar AJ, Ginsberg LE. Improving fat-suppressed T_2-weighted imaging of the head and neck with 2 fast spin-echo dixon techniques: initial experiences. AJNR Am J Neuroradiol 2009; 30:42–45.
10. Pipe JG. Motion correction with PROPELLER MRI: application to head motion and free-breathing cardiac imaging. Magn Reson Med 1999; 42:963–969.
11. Pipe JG, Gibbs WN, Li Z, Karis JP, Schar M, Zwart NR. Revised motion estimation algorithm for PROPELLER MRI. Magn Reson Med 2014; 72:430–437.
12. Chang Y, Pipe JG, Karis JP, Gibbs WN, Zwart NR, Schär M. The effects of SENSE on PROPELLER imaging. Magn Reson Med 2015; 74:1598–1608.
13. Huo D, Li Z, Aboussouan E, Karis JP, Pipe JG. Turboprop IDEAL: a motion-resistant fat-water separation technique. Magn Reson Med 2009; 61:188–195.
14. Weng D, Pan Y, Zhong X, Zhuo Y. Water–fat separation with parallel imaging based on BLADE. Magn Reson Imaging 2013; 31:656–663.
15. Schär M, Eggers H, Zwart NR, Chang Y, Bakhru A, Pipe JG. Dixon water–fat separation in PROPELLER MRI acquired with two interleaved echoes. Magn Reson Med 2016; 75:718–728.
16. Pruessmann KP, Weiger M, Scheidegger MB, Boesiger P. SENSE: sensitivity encoding for fast MRI. Magn Reson Med 1999; 42:952–962.
17. Busse RF, Hariharan H, Vu A, Brittain JH. Fast spin echo sequences with very long echo trains: design of variable refocusing flip angle schedules and generation of clinical T_2 contrast. Magn Reson Med 2006; 55:1030–1037.
18. Kojima S, Morita S, Ueno E, Hirata M, Shinohara H, Komori A. Aliasing artifacts with the BLADE technique: causes and effective suppression. J Magn Reson Imaging. 2011; 33:432–440.
19. Sasaki M, Inoue T, Tohyama K, Oikawa H, Ehara S, Ogawa A. High-field MRI of the central nervous system: current approaches to clinical and microscopic imaging. Magn Reson Med Sci 2003; 2:133–139.